# Conducting Organic Frameworks Based on a Main-Group Metal and Organocyanide Radicals

**ARTICLE** *in* CHEMISTRY - A EUROPEAN JOURNAL · MARCH 2013

Impact Factor: 5.73 · DOI: 10.1002/chem.201203422 · Source: PubMed

CHEMISTRY
A EUROPEAN JOURNAL

FULL PAPER

DOI: 10.1002/chem.201203422

# Conducting Organic Frameworks Based on a Main-Group Metal and Organocyanide Radicals

Zhongyue Zhang,[a] Hanhua Zhao,[a] Hirotaka Kojima,[b] Takehiko Mori,[b] and Kim R. Dunbar*[a]

**Abstract:** Reactions of the main-group cation $Tl^{I}$ with anions of 2,5-derivatives of TCNQ (TCNQ = 7,7,8,8-tetracyanoquinodimethane) have led to the isolation of a family of unprecedented semiconducting main-group-metal–organic frameworks, namely, $[Tl(TCNQX_2)]$, (X = H, Cl, Br, I). A comparison of single-crystal and powder X-ray diffraction data revealed the existence of a third polymorph of the previously reported material Tl(TCNQ)] and two distinct polymorphs of $[Tl(TCNQCl_2)]$, whereas only one phase was identified for $[Tl(TCNQBr_2)]$ and $[Tl(TCNQI_2)]$. These new results are described in the context of the structures of other known binary metal–TCNQ frameworks that display a variety of coordination environments for the central cation, namely, four-, six-, and eight-coordinate, and different arrangements of the adjacent TCNQ radicals—parallel versus perpendicular—in the stacked columns. The halogen substituents affect the structures and the properties of these compounds, owing to both steric and electronic effects as evidenced by the semiconducting properties of crystals of $[Tl(TCNQCl_2)]$ phase I, $[Tl(TCNQBr_2)]$, and $[Tl(TCNQI_2)]$, which correlate well with the distances of adjacent TCNQ radicals in the columns. 1D infinite Hückel model simulations of the band structures of $[Tl(TCNQCl_2)]$ phase I, $[Tl(TCNQBr_2)]$, and $[Tl(TCNQI_2)]$ were conducted with and without consideration of the $Tl^{I}$ cations, the results of which indicate that the charge mobility does not strictly occur in one dimension. The modulations of the band structures with various assumptions of the energy difference ($\Delta$) between the $Tl^{I}$ 6s orbital and the TCNQ LUMO orbital were calculated and are discussed in light of the observed properties.

**Keywords:** halogenated derivatives · main-group elements · semiconductors · polymorphism · thallium

## Introduction

The design of molecule-based materials with interesting electronic, optical, or magnetic properties is a central theme of modern materials-science research.[1] A particularly compelling goal in the pursuit of functional materials is the realization of new-generation memory devices with higher information densities and increased operation speeds. In this vein, considerable efforts are currently being directed towards the design and fabrication of tunable nanoscale materials and nanodevices.[2,3] One of the highly successful strategies in this area is the co-assembly of metal ions and organic radicals to prepare solids that exhibit electrical or magnetic bistability. In these materials, the metal donors (D) and the organic acceptors (A) are intimately organized into extended architectures that are often 1D in terms of the arrangement of the organic radicals. Pioneering studies of these hybrid systems include two particularly remarkable examples, namely, the room-temperature magnet $[V(TCNE)_x]\cdot y(solvent)$ ($x \cong 1$–2),[4] and the metallic conductor $[Cu(2,5\text{-DM-DCNQI})_2]$ (2,5-DM-DCNQI = 2,5-dimethyl-*N*,*N*′-dicyanoquinonediimine).[5]

One commonly used organocyanide acceptor is 7,7,8,8-tetracyanoquinodimethane (TCNQ), which undergoes two accessible reversible reductions and is air stable in the radical anion form. The versatility of the TCNQ molecule has led to its incorporation into a variety of important materials and devices with a seminal example being the charge-transfer salt $TTF^{\delta+}(TCNQ)^{\delta-}$ (TTF = tetrathiafulvalene) discovered in 1973 by Ferraris et al.[6] This is the first organic material to show metallic conductivity and the earliest example of an organic conductor that exhibits superconducting fluctuation phenomena.[7,8] The structural determination and band-structure analysis of TTF(TCNQ) sparked the development of the entire field of organic superconductors.

The 1970s witnessed the report of another extraordinary material, namely, [Cu(TCNQ)], by Cowan and co-workers who discovered that a sandwich device composed of Cu/[Cu(TCNQ)]/Al undergoes voltage-induced switching.[9,10] Much effort over the years has been directed at understanding the origin of the switching and the nature of the material, that is, the intrinsic structure and electronic properties, but a

[a] Z. Zhang, Dr. H. Zhao, Prof. K. R. Dunbar
Department of Chemistry, Texas A&M University
College Station, Texas 77842-3012 (USA)
Fax: (+1) 979-845-7177
E-mail: dunbar@mail.chem.tamu.edu

[b] H. Kojima, Prof. T. Mori
Department of Organic and Polymeric Materials
Tokyo Institute of Technology, Tokyo, 48824 (Japan)

Supporting information for this article is available on the WWW under http://dx.doi.org/10.1002/chem.201203422.

major hurdle has been the irreproducibility of the film devices prepared in different laboratories and under slightly different conditions.[10,11] Twenty years after the initial synthesis of [Cu(TCNQ)], efforts in our laboratories led to the realization that there are actually two polymorphs of this compound. We managed to grow very small crystals and determined their structures (Figure 1). The two different crystal-

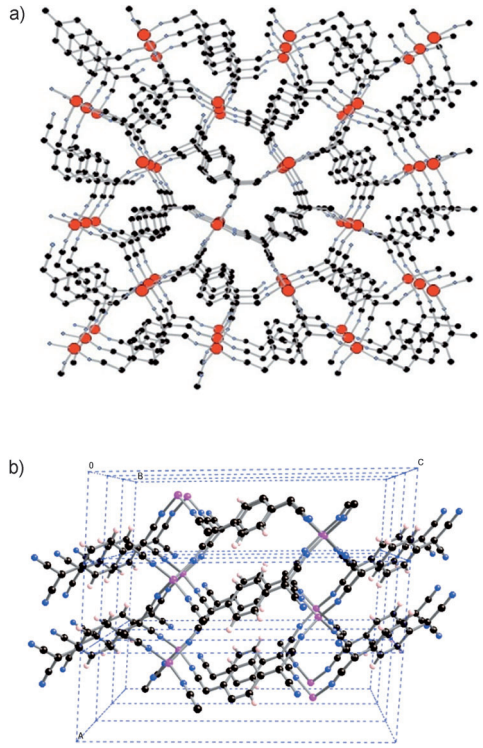


Figure 1. Structures of [Cu(TCNQ)] a) phase I and b) phase II drawn from X-ray coordinates.[12]

line forms exhibit dramatically different conductivities at room temperature, namely, 0.25 $S\,cm^{-1}$ for phase I and $1.3\times10^{-5}$ $S\,cm^{-1}$ for phase II.

The recognition of polymorphism in this material resolved the long-standing irreproducibility problem of device behavior which is due to the presence of a mixture of polymorphs in varying quantities.[12] This realization initiated a renewed interest in the mechanism of charge transfer and the fabrication of nanodevices.[13]

A major impediment to progress in this field of study has persisted since TCNQ was first prepared at Dupont in the 1960s,[14] namely, that a general understanding of the properties of simple binary $[M_x(TCNQ)_y]$ materials has been stymied due to a lack of structural information. The few binary TCNQ compounds for which structures have been determined exhibit extraordinary complexity and polymorphism. Subtle changes in the crystallization conditions, such as temperature or even humidity, can trigger a phase change. Moreover, facile interconversions between polymorphs under mild conditions lead to difficulties in the isolation and purification of materials. The best illustration of this point is the well-known polymorphism of the alkali-metal–TCNQ salts, $[M^+(TCNQ)^-]$ (M = Na, K, Rb, or Cs).[15] This series of segregated charge-transfer complexes was widely investigated in the 1970s owing to their unusual polymorphism and structurally related semiconducting behavior. One of the most well-studied materials, $[Rb^+(TCNQ)^-]$, was isolated as three different polymorphs from the same preparative procedure.[15b,16] Phase I (monoclinic, $P2_1/n$) and phase II (triclinic, $P\bar{1}$) exhibit, respectively, perpendicular and parallel arrangements of the stacks of the TCNQ radicals.[17,18] Phase III crystallizes in the $P4/n$ space group and is closely related to phase I in that it adopts a perpendicular stacking mode for the TCNQ radical units, but with a homogenous separation distance (3.33 Å) along the column instead of alternating shorter and longer separations (3.159 Å and 3.484 Å).[18] Interestingly, phase I undergoes a phase transition at 374 K and converts to phase III, with a conductivity increase of about 60%, and a decrease in activation energy (0.41–0.53 to 0.28–0.37 eV). Phase II exhibits much higher conductivity than phase I with a room-temperature conductivity of $10^{-2}$ $S\,cm^{-1}$ as compared with $10^{-5}$ $S\,cm^{-1}$.[15b]

As the previous case illustrates, the interconversion of polymorphs is accompanied by drastic changes in semiconducting behavior, but, in many cases, the structures have not been determined due to the difficulty in obtaining crystals of the rapidly precipitating phases; therefore an understanding of the factors that influence the properties is lacking.[15a] The dearth of structural information on known binary TCNQ materials with transition metals and the absence of main-group analogues is unfortunate, as such light-weight conductors hold great promise for device applications, especially if they can be properly tuned as to their steric and electronic properties with substituents on the TCNQ radical. In this vein, our group recently initiated a broad investigation of various 2,5-halogenated TCNQ derivatives with the goal of obtaining single-crystal phases and observing enhanced conducting properties.[19] Indeed, these studies have led to new semiconductors with previously unknown structures, including $[Cu(TCNQCl_2)]$ and $[Cu(TCNQBr_2)]$,[20] with the chloro derivative setting the record among the conducting 1:1 $[M^+(TCNQ)^-]$ salts with a room-temperature conductivity of 1.15 $S\,cm^{-1}$. An analysis of the structure–property relationships revealed that the steric and electronic effects of the substituent has a profound influence on the structures and properties as compared to the original [Cu(TCNQ)] phases.

Given the promising discoveries over the decades with s- and d-block binary TCNQ phases, we decided to expand the field of TCNQ materials by exploring the chemistry of the "pseudo-alkali-metal" main-group element thallium. Thallium prefers the monovalent oxidation state and exhibits similar chemical properties to alkali-metal cations. We reasoned that because the electronegativity of Tl is 2.04, much higher than that of any alkali metal, partial charge transfer may occur from the TCNQ radical anion to the $Tl^I$ cation and lead to a decrease in the band gap. As a backdrop for these

studies, we noted that [Tl(DM-DCNQI)$_2$] has been reported to exhibits a degree of electron-density transfer from DCNQI, a conclusion that is supported by a Knight shift in the $^{205}$Tl NMR spectrum at 85 K.[21] In addition, unlike alkali metals, Tl$^{I}$ possesses a stereoactive lone pair, which leads to different structures than those of alkali metals[22] and may also alter the semiconducting behavior. With these details in mind, we prepared the compound [Tl(TCNQ)], which was found to exist as two polymorphs with dramatically different conducting properties. Moreover, a surprising unprecedented room-temperature crystal-to-crystal phase transition was observed to occur between the polymorphs in a humid environment.[23]

Given these aforementioned fascinating results, we undertook the syntheses of thallium(I) materials with the 2,5-substituted derivatives, TCNQX$_2$ (X = Cl, Br, I). Herein we report the new semiconductors [Tl(TCNQX$_2$)] along with their structures and a theoretical analysis and comparisons to the related TCNQ phases, which have been published, in part, in a previous communication.[23]

## Results and Discussion

**X-ray crystallographic analyses**: *[Tl(TCNQCl$_2$)] phase I (**1**), and [Tl(TCNQBr$_2$)] (**3**)*: Single-crystal X-ray data collected on compounds **1** and **3** revealed that these isostructural compounds crystallize in the monoclinic space group *P*2/*c*. The projections in the *ab* and *bc* planes are depicted in Figure 2. The Tl$^{I}$ ions reside in a distorted cubic environment with a coordination number of eight and are arranged in chains positioned between the TCNQ layers. The Tl···Tl separations are 3.42(1) Å (**1**) and 3.41(1) Å (**3**), which are less than the Tl···Tl van der Waals contact of 3.92 Å. The TCNQX$_2^-$ radical anions are arranged in a columnar stack with the two halogen atoms on alternating sides of the stack as can be clearly seen in Figure 2a and b. One interesting feature is that the adjacent TCNQ radicals along the stack are not perfectly parallel (dihedral angle = 0.5° for [Tl(TCNQCl$_2$)] and 1.5° for [Tl(TCNQBr$_2$)]). The average stacking distances are 3.30(1) Å for TCNQCl$_2^-$ and 3.28(1) Å for TCNQBr$_2^-$. Given the non-zero dihedral angles between adjacent planar radicals, the π–π interactions are expected to be less than for a perfect parallel case.

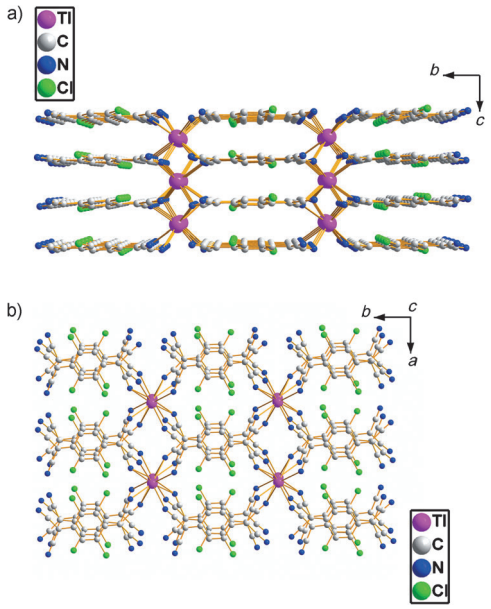


Figure 2. Views of the structure of [Tl(TCNQCl$_2$)] phase I (**1**) in a) the *bc* plane and b) the *ab* plane ([Tl(TCNQBr$_2$)] (**3**) adopts the same structure).

*[Tl(TCNQI$_2$)] (**4**)*: Compound **4** crystallizes in the monoclinic space group $P\bar{1}$ with a different structure than the others in this family. The material adopts a 2D motif in which the Tl$^{I}$ metal ions are situated in layers surrounded by four TCNQI$_2^-$ radical anions. The projection in the *bc* plane (Figure 3a) reveals that the TCNQI$_2^-$ groups are arranged

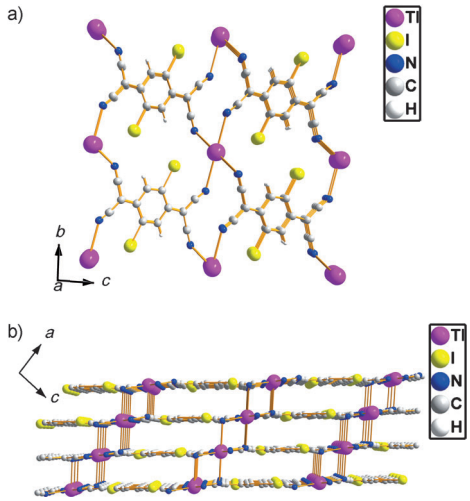


Figure 3. Views of the structure of [Tl(TCNQI$_2$)] (**4**) in a) the *bc* plane and b) the *ac* plane.

with the iodine substituents pointing in the same direction. Owing to the bulk of the iodine atoms, the TCNQI$_2$ units are in a slipped-stacked arrangement as can be seen in Figure 3b; the I···I and Tl···Tl separations are identical at 4.12 Å. The six-coordinate Tl$^{I}$ ions are in a distorted octahedral environment. The Tl–N bonds lengths within the plane are in the range of 2.91–2.97 Å and the Tl···N bond lengths between the planes is 3.20 Å (Figure S1 in the Supporting Information). The TCNQI$_2^-$ radical anions are evenly spaced in the column with a stacking distance of 3.28(1) Å.

*[Tl(TCNQ)] phase III (**5**)*: Crystals of a new phase of the material were unexpectedly obtained during an attempt to prepare a bulk sample of [Tl(TCNQ)] phase I. When the reaction between TlPF$_6$ and (Bu$_4$N)$^+$TCNQ$^-$ is performed in dry acetonitrile, the result is a dark-purple powder for which

the powder XRD pattern is very similar to the simulated spectrum obtained from the single-crystal data of [Tl(TCNQ)] phase I.[23] Surprisingly, however, unlike phase I the new material does not undergo a phase transition when suspended in water or methanol for several days. By using a thin-tube diffusion method, tiny crystals of **5** were obtained and structurally characterized at the Advanced Photon Source facility at Argonne National Lab. The structure is nearly identical to [Tl(TCNQ)] phase I in the stacking mode and with the space group $P2_1/c$ (Figure 4a,b and Table 1), but the dimensions of the unit cell are slightly decreased. For the new phase, the cell parameters are $a=6.987$ (1), $b=12.332(3)$, $c=12.947(3)$ Å, $\beta=97.75(3)°$, $V=1105.9(4)$ Å$^3$, whereas the same parameters for the original structure of [Tl(TCNQ)] phase I are $a=7.165(1)$, $b=12.441(3)$, $c=12.999(3)$ Å, $\beta=98.03(1)°$, $V=1148.0(4)$ Å$^3$. The decrease in volume leads to an increased overlap of the frontier orbitals and stronger interactions between adjacent TCNQ radicals. This subtle, but important difference, leads to increased stability of phase III with no further phase transition observed. The separations between the adjacent TCNQ radicals of 3.13 and 3.29 Å, which is evidence of a strong dimerization, support this conclusion.

Table 1. Pertinent crystallographic parameters and data for compounds **1**, **3**, **4**, and **5**.

| Compound | **1** | **3** | **4** | **5** |
|---|---|---|---|---|
| formula | $C_{12}H_2N_4Cl_2Tl$ | $C_{12}H_2N_4Br_2Tl$ | $C_{12}H_2N_4I_2Tl$ | $C_{12}H_4N_4Tl$ |
| $F_w$ [g mol$^{-1}$] | 477.46 | 566.36 | 660.37 | 408.57 |
| crystal size [mm$^3$] | 0.40×0.30×0.20 | 0.34×0.24×0.16 | 0.33×0.30×0.22 | 0.08×0.02×0.01 |
| crystal system, SG | monoclinic, $P2/c$ | monoclinic, $P2/c$ | monoclinic, $P\bar{1}$ | monoclinic, $P2_1/c$ |
| $a$ [Å] | 7.538(2) | 7.756(2) | 4.120(1) | 6.987(1) |
| $b$ [Å] | 11.804(2) | 11.640(2) | 8.494(2) | 12.332(3) |
| $c$ [Å] | 6.843(1) | 6.813(1) | 9.099(2) | 12.947(3) |
| $\alpha$ [°] | 90 | 90 | 91.12(3) | 90 |
| $\beta$ [°] | 96.85(3) | 97.72(3) | 95.55(3) | 97.75(3) |
| $\gamma$ [°] | 90 | 90 | 95.74(3) | 90 |
| $V$ [Å$^3$] | 604.59(7) | 609.47(3) | 315.26(4) | 1105.4(6) |
| $Z$ | 2 | 2 | 1 | 4 |
| $\rho_{calcd}$ [g cm$^{-3}$] | 2.645 | 3.086 | 3.478 | 2.454 |
| $\mu$ ($Mo_{K\alpha}$) [mm$^{-1}$] | 0.711 | 0.711 | 0.711 | 0.413(synchrotron) |
| collected reflns | 6610 | 1456 | 2942 | 2892 |
| unique reflns | 1468 | 1456 | 1429 | 2892 |
| reflns with $I>2\sigma(I)$ | 1350 | 1362 | 1255 | 1980 |
| parameters | 47 | 88 | 88 | 69 |
| $R$(int) | 0.0359 | 0.0309 | 0.0297 | 0.0642 |
| $R1$[a] | 0.0277 | 0.0485 | 0.0393 | 0.0877 |
| $wR2$[b] | 0.1159 | 0.1178 | 0.0919 | 0.0823 |
| GOF | 1.001 | 1.150 | 1.051 | 1.054 |

[a] $R1=\Sigma||F_o|-|F_c||\Sigma|F_o|$. [b] $wR2=[\Sigma[w(F_o^2-F_c^2)^2]/\Sigma[w(F_o^2)^2]]^{1/2}$.

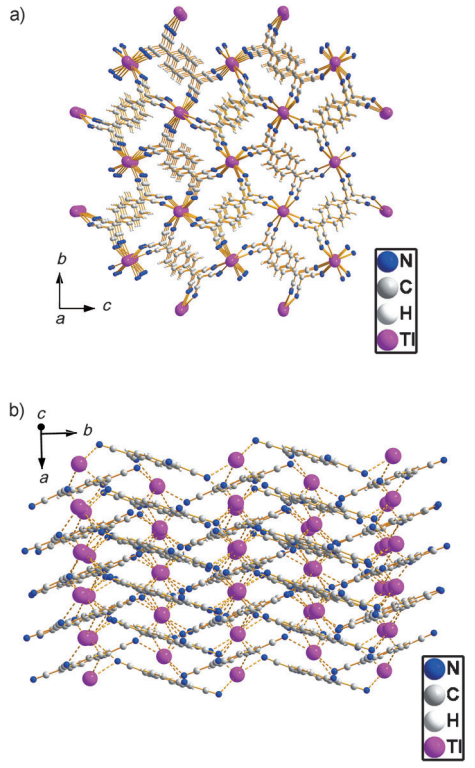


Figure 4. Views of [Tl(TCNQ)] phase III (**5**) prepared in $CH_3CN$ in the a) *bc* and b) *ab* planes.

**Structural comparison of the 1:1 [M(TCNQ)] phases**: As mentioned in the previous section, the co-assembly of $Tl^I$ cations and TCNQ radicals results in a variety of structure types. To put these new results into perspective, it is instructive to examine the diversity of the structures of the 1:1 [M(TCNQ)] materials (excluding the alkali metals) depicted in Figure 5.[12,20,23,27] The particular architecture is characterized by the coordination number of the metal cations and the orientation motif and stacking of the TCNQ radicals A four-coordinate environment is observed for the $Cu^I$ and $Ag^I$ materials, with a perpendicular arrangement of the TCNQ ligands for [Cu(TCNQ)] phase I and [Ag(TCNQ)] phase II. In contrast, [Cu(TCNQ)] phase II and [Cu(TCNQX$_2$)] (X = Cl, Br) adopt a parallel packing mode for the TCNQ moiety with different relative positions of adjacent columns (non-coplanar versus coplanar). The $Tl^I$ ion is in an eight-coordinate environment in [Tl(TCNQ)] phase I and II as well as in [Tl(TCNQX$_2$)] (X = Cl, Br) with perpendicular, parallel/non-coplanar, and parallel/coplanar arrangements of the TCNQ radicals, respectively. An exceptional case is the six-coordinate [Tl(TCNQI$_2$)], which adopts a layered architecture, presumably as a result of the steric effect of the iodine substituents.

**Polymorphism in binary M(TCNQ) phases**: An overarching theme in metal binary TCNQ compounds is that of polymorphism. Slightly different preparation conditions can lead

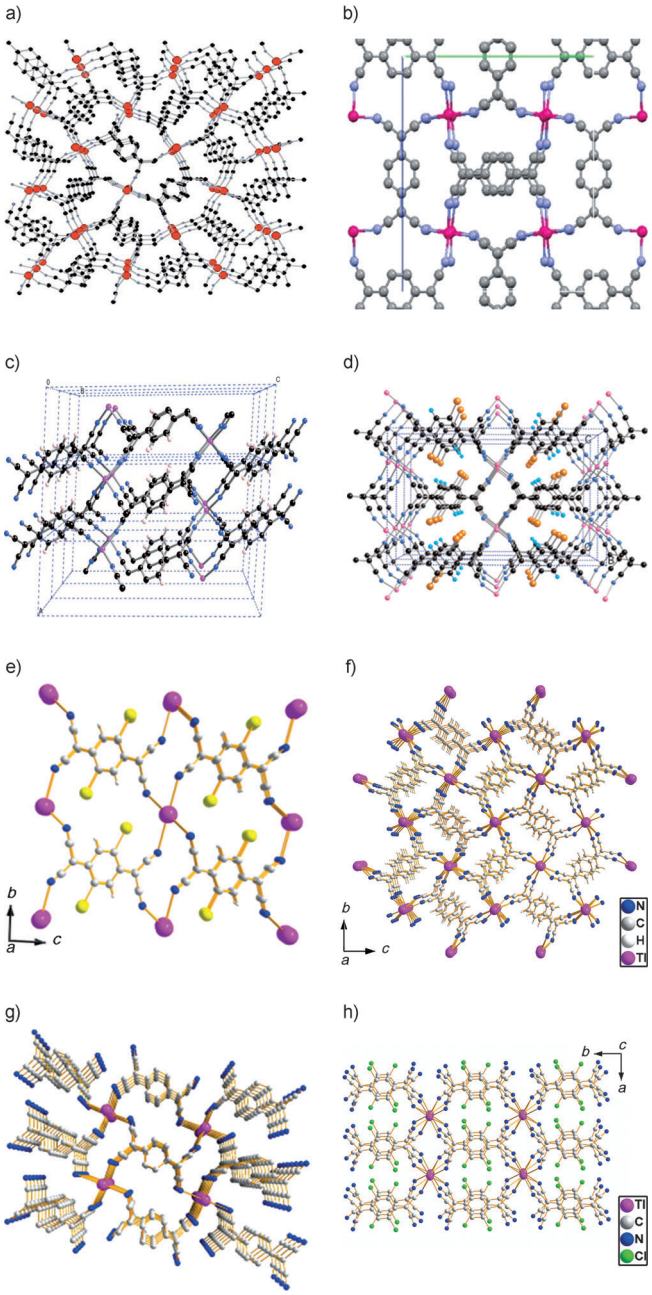


Figure 5. Structures of known polymorphs of binary [M(TCNQ)] phases determined by single-crystal X-ray diffraction: a) four-coordinate type I: [Cu(TCNQ)] phase I b) four-coordinate type I: [Ag(TCNQ)] phase II, c) four-coordinate type II: [Cu(TCNQ)] phase II, d) four-coordinate type III: [Cu(TCNQX$_2$)] (X = Cl, Br), e) six coordinate: [Tl(TCNQI$_2$)], f) eight-coordinate type I: [Tl(TCNQ)] phase I and III, g) eight-coordinate type II: [Tl(TCNQ)] phase II, h) eight-coordinate type III: [Tl(TCNQX$_2$)] (X = Cl, Br).

to materials for which the properties are vastly different. For example, the initial kinetic polymorph of [Cu(TCNQ)], which is an excellent semiconductor, undergoes a first-order phase transition in warm acetonitrile without apparent dissolution to form a thermodynamic phase which is nearly insulating.[12] The more ionic compounds with alkali-metal ions form a polymorph that undergoes a secondary transition to a spin-Peierls phase at a critical temperature (348 K for [Na(TCNQ)], 395 K for [K(TCNQ)], 381 K for [Rb(TCNQ)], and 210 K for [Cs(TCNQ)]), with a concomitant magnetic phase transition and a change in semiconducting behavior.[15,28–30] Given these issues with polymorphism, it is important to compare the powder X-ray pattern of products from bulk reactions with the simulated pattern from the corresponding single-crystal data. Recently we communicated a preliminary report of the preparation of two distinct [Tl(TCNQ)] polymorphs, which constitute another entirely new class of 1:1 [M(TCNQ)] polymorphs. Single crystals of [Tl(TCNQ)] phase I are obtained by thin tube layering of a solution of [Li(TCNQ)] in MeOH and $TlPF_6$ in $H_2O$/MeOH. A microcrystalline form of [Tl(TCNQ)] phase II can be prepared by stirring [Li(TCNQ)] and $TlPF_6$ in water for 2 h.[23] The difference between the powder X-ray diffraction patterns of the bulk powder and the data simulated from the corresponding single crystals revealed the existence of polymorphs.

Interestingly, although two polymorphs of [Tl(TCNQCl$_2$)] were obtained (Figure 6a), only one phase of [Tl(TCNQBr$_2$)] was detected irrespective of the conditions (Figure 6b). All attempted bulk preparations of [Tl(TCNQI$_2$)] led to amorphous powders. Because the electron-withdrawing properties of the halogen substituents are similar according to the first-reduction potentials ($E_{1/2}$ = 0.48 V for $TCNQCl_2$, 0.49 V for $TCNQBr_2$ and 0.46 V for $TCNQI_2$ referenced to the Ag/AgCl eletrode), it is reasona-

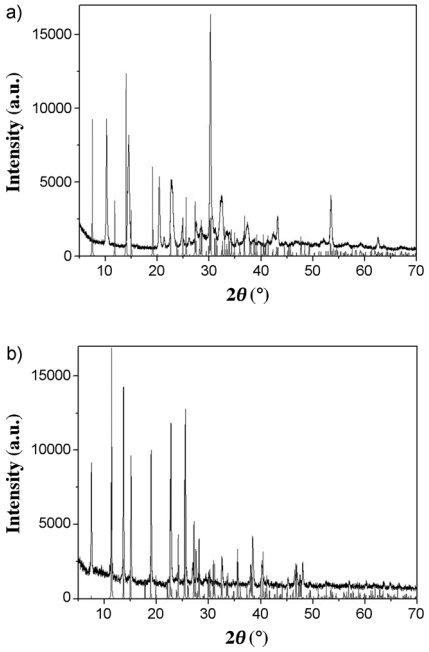


Figure 6. Powder X-ray data of a) a bulk sample of phase II of [Tl(TCNQCl$_2$)] (upper trace) overlaid with data simulated from single crystals of phase I (lower trace), indicating that they are different phases, and of b) a bulk sample of [Tl(TCNQBr$_2$)] (upper trace) overlaid with the simulation from the single crystal data (lower trace), verifying that the two phases are identical.

ble to expect that the stacking models of TCNQ moieties are primarily dictated by the steric effect of halogen atoms. For example, apart from the compound that is isostructural with [Tl(TCNQBr$_2$)], a second phase of [Tl(TCNQCl$_2$)] was discovered; this hints at improved flexibility in terms of stacking options available for the chlorine derivative. In the case of [Tl(TCNQI$_2$)], the much larger iodine atoms apparently lead to a less stable crystal-packing arrangement and, as a result, only amorphous solids were obtained, despite many attempts to grow crystals.

**IR spectroscopy**: Infrared spectroscopy is a useful technique for characterizing TCNQ charge-transfer salts, especially with respect to distinguishing the presence of TCNQ in its various redox states. The pertinent data for known binary phases as well as the new [Tl(TCNQX$_2$)] compounds (X = H, Cl, Br, I) are provided in Table 2. Compounds **1** and **3** exhibit $\nu$(C≡N) stretching modes at 2143, 2132, and 2121 cm$^{-1}$ and at 2185, 2169, and 2154 cm$^{-1}$, respectively; these values are similar to the copper derivatives [Cu(TCNQX$_2$)] (X = Cl, Br). The similarity of the $\nu$(C≡N) modes indicates an analogous coordination environment for the cyanide groups, which we know to be the case for **1** and **3**. Compound **2**, however, exhibits an intense and sharp $\nu$(C≡N) absorption at 2183 cm$^{-1}$ with a shoulder at 2154 cm$^{-1}$. In the case of compound **4**, the $\nu$(C≡N) modes appear as intense and broad absorptions at 2176 cm$^{-1}$ and 2145 cm$^{-1}$. The differences in the infrared spectra of **1** and **2** are a result of polymorphism, as found for [Tl(TCNQ)] phase I and II compounds as well. In all cases, the data support the conclusion of one-electron-reduced radicals of the TCNQ molecules.

Table 2. IR spectral data for [Tl(TCNQX$_2$)] compounds.

| | $\nu$(C≡N) [cm$^{-1}$] | $\delta$(C–H) [cm$^{-1}$] |
|---|---|---|
| [Tl(TCNQ)] phase I[a] | 2181, 2164, 2151 | 823 |
| [Tl(TCNQ)] phase II[a] | 2180, 2149 | 822 |
| [Tl(TCNQ)] phase III (**5**) | 2182, 2165, 2151 | 823 |
| [Tl(TCNQCl$_2$)] phase I (**1**) | 2143, 2132, 2121 | 834 |
| [Tl(TCNQCl$_2$)] phase II (**2**) | 2183, 2154 | 835 |
| [Tl(TCNQBr$_2$)] (**3**) | 2185, 2169, 2154 | 845 |
| [Tl(TCNQI$_2$)] (**4**) | 2176, 2145 | 846 |

[a] Ref. [23].

It is also instructive to examine the out-of-plane $\delta$(C–H) bending mode, which is very sensitive to the oxidation state of the TCNQ moiety. The $\delta$(C–H) modes appear at 834, 835, 845, and 846 cm$^{-1}$ for **1**, **2**, **3** and **4**, respectively, data that confirm the existence of the radical form of the TCNQ moiety in the compound. In terms of comparison, the $\delta$(C–H) modes of TCNQCl$_2$, TCNQBr$_2$, and TCNQI$_2$ appear at 848, 874, and 870 cm$^{-1}$ and the bending modes for the reduced lithium salt occur at 828, 847, and 846 cm$^{-1}$.

**Conductivity data and relationship to structural parameters**: Most binary TCNQ salts are semiconductors due to the stacking interactions in columns of TCNQ radicals, the existence of which leads to overlap between the SOMO and the LUMO of adjacent radicals; this situation facilitates electron hopping. Typically the band structure and conductivity data can be predicted by taking the charge, stacking motif, and structural parameters of the material into account. For example, we discovered that one polymorph of [Tl(TCNQ)] phase I exhibits alternating distances between both the adjacent TCNQ molecules (3.16(1) and 3.35(1) Å) and the Tl$^{I}$ ions (3.63(1) and 3.45(1) Å), a signature of a typical spin-Peierls material in which adjacent TCNQ radicals are partially dimerized. Antiferromagnetic interactions between the spins lead to a secondary gap in the energy band and therefore a decrease in the conductivity properties. In contrast, [Tl(TCNQ)] phase II adopts a homogeneous stacking motif with uniform distances between the TCNQ radicals (3.22 (1) Å) and the Tl$^{I}$ cations (3.79 (1) Å). As a consequence of the regular structure, the conductivity of phase II is expected to be much higher than for the first polymorph of [Tl(TCNQ)]. Indeed, the pressed pellet data revealed that phase I exhibits a nearly insulating room-temperature conductivity of $2.4\times10^{-4}$ S cm$^{-1}$, whereas phase II exhibits a much higher room-temperature conductivity of $5.4\times10^{-1}$ S cm$^{-1}$.

Crystals of **1**, **3**, and **4** were subjected to single-crystal conductivity measurements by the two-probe method. The temperature dependent conductivity plotted in Figure 7 clearly indicate that all three compounds are semiconductors. The room temperature conductivities of **1** and **3** are nearly the same ($9.3\times10^{-3}$ S cm$^{-1}$ and $2.1\times10^{-3}$ S cm$^{-1}$), which is not surprising given their structural similarity. Compound **4** exhibits a slightly higher room temperature conductivity at $2.9\times10^{-2}$ S cm$^{-1}$. The energy gaps were obtained by fitting the curves to an Arrhenius expression and are 172, 85, and 160 meV for **1**, **3**, and **4**, respectively.

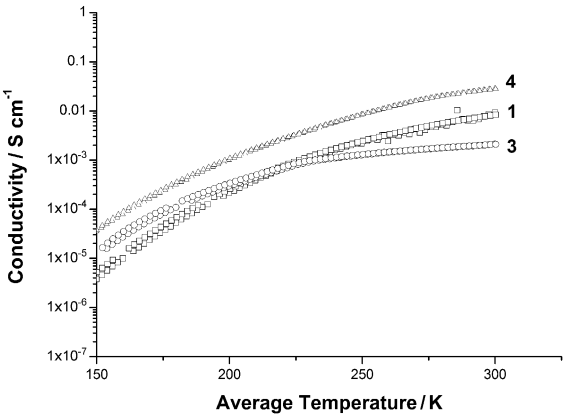


Figure 7. Temperature-dependent conductivity data obtained on single crystals of **1**, **3**, and **4**.

Table 3 contains a compilation of structural parameters and properties for all of the [Tl(TCNQX$_2$)] (X = H, Cl, Br, I) phases. Except for [Tl(TCNQ)] phase I, the compounds

Table 3. Selected structural and conductivity data for the series [Tl(TCNQX$_2$)] (X = H, Cl. Br, I).

| | Tl···Tl distance [Å] | TCNQ···TCNQ distance [Å] | $\sigma$ (RT) [S cm$^{-1}$] |
|---|---|---|---|
| [Tl(TCNQ)] phase I | 3.45/3.63 | 3.16/3.35 | $2.4\times10^{-4}$ |
| [Tl(TCNQ)] phase II | 3.79 | 3.22 | $5.4\times10^{-1}$ |
| Tl(TCNQ) phase III (**5**) | 3.39/3.61 | 3.13/3.29 | $2.8\times10^{-4}$ |
| [Tl(TCNQCl$_2$)] phase I (**1**) | 3.42 | 3.30[a] | $9.3\times10^{-3}$ |
| [Tl(TCNQBr$_2$)] (**3**) | 3.41 | 3.28[a] | $2.1\times10^{-3}$ |
| [Tl(TCNQI$_2$)] (**4**) | 4.10 | 3.28 | $2.9\times10^{-2}$ |

[a] Average distance, see structural-description section. Powder pressed pellets were used for [Tl(TCNQ)] phase I, II, and III and single crystals for **1**, **3**, and **4**.

adopt a stacking model with a uniform stacking distance between the TCNQ moieties and no dimerization of the TCNQ radicals and they exhibit higher conductivities than the compounds with non-uniform stacks and dimerization of the TCNQ radicals. If one compares [Tl(TCNQ)] phase II with the halogen derivatives **1**, **3**, and **4**, it is reasonable to expect the longer distances between the adjacent TCNQ radicals to result in less overlap of the frontier orbitals, hence lower conductivities than for [Tl(TCNQ)] phase II. This logic does not actually prevail, however, as the trend in the stacking distances is [Tl(TCNQ)] phase II < **4**≅**3** < **1**, but the observed conductivities are [Tl(TCNQ) phase II > **4** > **1** > **3**.

**Band structure calculations**: Given that the valence-shell electrons of the Tl$^{I}$ metal ion are 6s electrons that constitute an inert lone pair, they are expected to lead to much weaker interactions than 3d transition metal ions,[31] for example, Cu$^{I}$ with organocyanide acceptors.[5,12,38] Nevertheless spin-density transfer from the ligand to the Tl$^{I}$ ion has been reported in the case of [Tl(DM-DCNQI)$_2$].[21] Because the Tl$^{+}$ compounds are similar to the K$^{+}$ counterparts,[32,33] the alkali-metal–TCNQ salts are more suitable as a theoretical model for a band-structure study of the series [Tl(TCNQX$_2$)] (X = H, Cl, Br, I) than the transition-metal analogues. As a "first-principles" approach, these materials can be treated as "radical-only" charge carriers, which implies that the contributions to the conductivity can be described solely by an extended Hückel model of the TCNQ columns of charge carriers.[34–36]

The approach of our simulation was to initially treat the [Tl(TCNQ)] species as "TCNQ-only" semiconductors, that is, to neglect the contribution of the 6s orbitals of the Tl$^{I}$ cation to evaluate the interaction between adjacent radicals. The 6s orbital contribution was then introduced in the next phase of the calculation as a perturbation of the major 1D conducting feature. In the first step, the intra-stack transfer integrals between adjacent TCNQ radicals were calculated to be $t_c$ = 156 and 170 meV for compounds **1** and **3**, respectively (Figure 8a). These values are in agreement with the reported estimations of transfer integrals in TCNQ chains.[37] The value for **4** was similarly evaluated to be 145 meV (Figure 8b). The largest interchain transfer integrals are less than 4 meV; this result implies that these compounds are highly 1D. Indeed, the calculated bandwidths of the TCNQ stacks are 0.62, 0.68, and 0.58 eV for **1**, **3**, and **4**, respectively.

The transfer integrals between the TCNQ LUMO and Tl6s orbitals were evaluated and the values $t_1$–$t_4$ are listed in captions in Figure 8. The metal–organic transfers are approximately half (50–70 meV) of those within the TCNQ radical stacks. These values are approximately the same as the reported p–d interactions (53.8 meV) for [Cu(DMDCNQI)$_2$] (DMDCNQI = *N*,*N*′-dimethyldicyanoquinonediimine).[38] By adopting these transfer integrals, the tight-binding energy band depicted in Figure 9 was obtained for **1**, and the energy band of **3** is

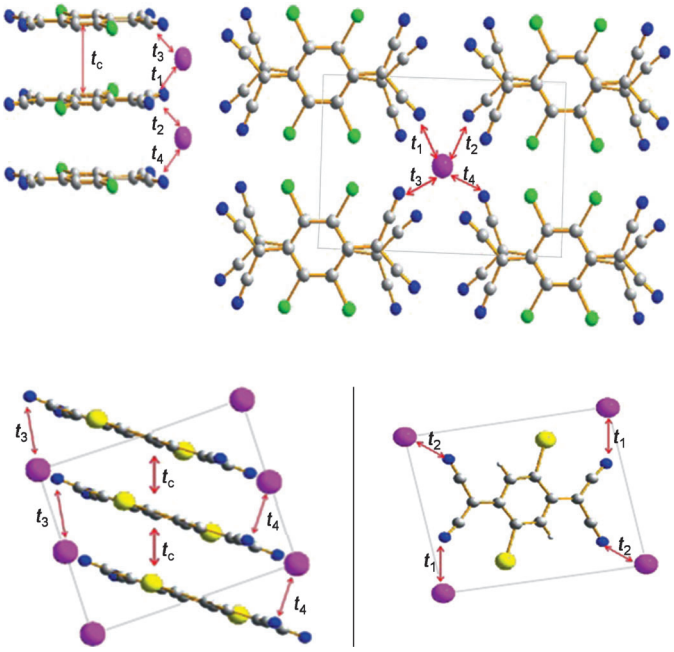


Figure 8. a) Transfer integral diagram for **1** (**3** adopts the same diagram). The $t_c$ value represents the intra-stack transfer integral between adjacent TCNQ molecules, and is $t_c$ = 156 meV for **1** and 170 meV for **3**. The $t_{1-4}$ values represent the transfer integrals between the Tl6s orbital and the LUMO of the TCNQ molecule, and are $t_{1-4}$ = −48, 71, −70, and 88 meV for **1** and −87, 70, −71, and 39 meV for **3**. The types of transfers are restricted by the symmetry of the structure. b) Transfer integral diagram for **4**, for which $t_c$ = 145 meV and $t_{1-4}$ = −7, 26, 57, and −69 meV.

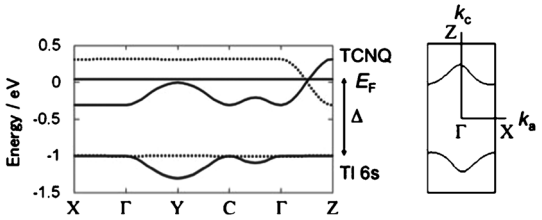


Figure 9. Tight-binding energy band (left) and Fermi surface modulation (right) for **1**, including the TCNQ LUMO and the Tl6s orbitals. The transfer integrals are taken from the caption for Figure 8. Solid and dashed curves represent the band dispersions at $k_c$ = 0 and $\pi/c$, respectively. C represents the position ($\pi/a$, $\pi/b$, $k_c$).

practically the same. The large dispersion of ΓZ at the right end of Figure 9 comes from the 1D TCNQ band. We have assumed that the nearly flat Tl6s band is located at $\Delta = 1$ eV below the TCNQ band. Although the TCNQ chain is composed of two molecules in the repeat unit of the column (Figure 2), the stacking is uniform owing to the glide symmetry along the *c* axis. As a consequence, the energy bands are degenerate at the $k_c = \pi/2c$ point, namely, the midpoint of Γand Z in Figure 9. We can represent it as the solid curve in the extended-zone scheme, but the dashed curve crosses the solid curve at $k_c = \pi/2c$ owing to this degeneracy. The dashed curve does not show any dispersion in the $k_x$ and $k_y$ directions as indicated in the right part of Figure 9, whereas the solid curve shows considerable dispersion in the ΓYC line. The dispersion is a mirror image of the Tl 6s band, indicating that it is mediated by the Tl 6s orbitals. Because the metal–organic interactions bridge the TCNQ molecules along the *x* and *y* axes (Figure 8), the dispersion appears in these directions. The Fermi surface is considerably modulated, however, as depicted in Figure 9. Because even [Tl(DMDCNQI)$_2$] undergoes a Peierls-like transition,[21] the metal orbital hybridization of Tl is expected to be less than that of Cu.[38] Accordingly, the actual Δ is expected to be slightly larger than this value, and the Tl6s hybridization is not so extensive as to destroy the 1D character of the TCNQ chain. Nevertheless, the Tl6s mediates the interchain interaction to some extent, and this is likely to be responsible for the uniform chain arrangement in the Tl salts. If there is no hidden or diffuse dimerization, these energy bands lead to a Mott insulating state owing to the half-filled nature. We can attribute the comparatively high conductivities of the present compounds ($10^{-3}$–$10^{-2}$ S cm$^{-1}$) to the Mott insulating state. This finding in in contrast to examples with obvious dimerization observed in such materials as [Ag(TCNQ)] phase I and [Tl(TCNQ)] phase I ($10^{-4}$ S cm$^{-1}$).

Figure 10 depicts the LUMO components of the $TCNQX_2$ radicals and illustrates the contribution of the halogen substituents. In addition to the stacking arrangement, the electron-withdrawing effect of different halogen groups affects the conductivity of the material as well through involvement of the LUMO of the radical, which alters the energy gap.

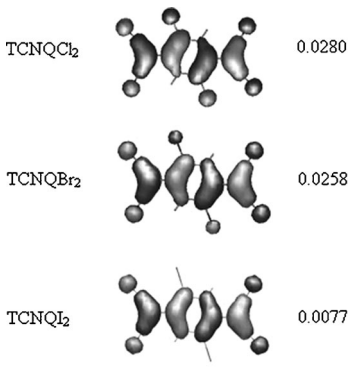


Figure 10. LUMO diagrams of $TCNQX_2^-$ radicals with the indicated Mulliken charges on the halogen atom.

As mentioned earlier, compounds **1** and **3** exhibit analogous stacking patterns with 3.30 and 3.28 Å separations, respectively. Because the LUMO of **1** has a bigger component from Cl atomic orbitals (Mulliken charge = 0.0280) than **3** with Br atomic orbitals (Mulliken charge = 0.0258), the electron-withdrawing halogen groups in **1** lead to a higher electron-accepting LUMO, hence an increased room-temperature conductivity.

## Conclusion

A new family of main-group molecule-based semiconductors, [Tl(TCNQX$_2$)] (X = H, Cl, Br, I), has been obtained and subjected to a comprehensive investigation of their structures and properties. Single-crystal conductivity measurements revealed that the derivatives exhibit room-temperature conductivities in the range $10^{-2}$–$10^{-3}$ S cm$^{-1}$, which falls into the range of semiconductors. A comparison of the metrical parameters of the structures and the conductivities leads to predictions of the stacking model and the separation distances of the TCNQ radicals which are supported by the band-structure simulations. The new results add to a relatively small database of structure–property correlations for TCNQ binary conductors and, importantly, introduces the first examples with main-group element materials, an entirely unexplored area of hybrid inorganic–organic donor–acceptor solids.

## Experimental Section

**General considerations**: All reactions and manipulations were carried out under a dry nitrogen atmosphere. Deionized water was boiled and purged with nitrogen for 1 h to remove dissolved oxygen. Dry methanol was obtained by distillation over Mg turnings under a nitrogen atmosphere. Acetonitrile was dried over 3 Å molecular sieves and distilled under an atmosphere of nitrogen prior to use. The TCNQ sample was purchased from TCI and $TlPF_6$ was supplied by Aldrich. The derivatives $TCNQX_2$ (X = Cl, Br, I) and their $Li^+$ and $[Bu_4N]^+$ salts were synthesized according to literature methods.[14] Elemental analyses were performed by Atlantic Microlab on bulk prepared powders. Single-crystal X-ray data were collected on a Bruker-AXS APEX-II CCD 3-circle X-ray diffractometer with the exception of [Tl(TCNQ)] phase III data which were collected at the synchrotron facility of ChemMatCars at Advanced Photon Source, Argonne National Lab. Powder X-ray data were collected on a Bruker D8-Focus Bragg–Brentano X-ray powder diffractometer. Variable-temperature conductivity measurements over the range 150–300 K were obtained on a Quantum Design model MPMS SQUID magnetometer by using gold paste to connect two 15 μm diameter gold wires to each end of the long axis of the needle-shape single crystals, which is the (011) face of the single crystal and the direction of columnar stacking of TCNQ radicals. Infrared spectra were recorded as Nujol mulls between KBr plates with a Nicolet IR/42 FT-IR spectrometer.

**Syntheses**: *[Tl(TCNQCl$_2$)] phase I (**1**)*: A quantity of [Li(TCNQCl$_2$)] (0.028 g, 0.1 mmol) was dissolved in methanol (10 mL) and $TlPF_6$ (0.035 g, 0.1 mmol) was dissolved in a 15 mL mixture of methanol/water (2:1 v/v). The two solutions were slowly diffused into each other by layering in a thin tube with a 6 mm outside diameter. Dark-purple needle-shaped crystals formed over the course of two days.

*[Tl(TCNQCl$_2$)] phase II (**2**)*: Samples of [Li(TCNQCl$_2$)] (0.028 g, 0.1 mmol) and $TlPF_6$ (0.035 g, 0.1 mmol) were dissolved in methanol

(10 mL) and the mixture was stirred for 2 h. The resulting precipitate was collected by filtration and dried in vacuo. Yield 0.038 g, 80%; elemental analysis calcd (%) for $C_{12}H_2N_4Cl_2Tl$: C 30.19, H 0.42, Cl 14.85, N 11.73; found: C 30.01, H 0.24, Cl 14.59, N 11.70.

*[Tl(TCNQBr$_2$)] (**3**)*: Separate samples of [LiTCNQBr$_2$] (0.037 g, 0.1 mmol) and $TlPF_6$ (0.035 g, 0.1 mmol) were dissolved in methanol (10 mL) and the mixture was stirred for 2 h. The resulting precipitate was collected by filtration and dried in vacuo. Yield 0.052 g, 93%; elemental analysis calcd (%) for $C_{12}H_2N_4Br_2Tl$: C 25.45, H 0.36, Br 28.22, N 9.89; found: C 25.57, H 0.32, Br 28.14, N 9.94. Single crystals were obtained by slow diffusion of [Li(TCNQBr$_2$)] (0.051 g, 0.1 mmol) in methanol (10 mL) and $TlPF_6$ (0.035 g, 0.1 mmol) into a 15 mL mixture of methanol/water (2:1 v/v) in a 6 mm O.D. thin tube. Dark-purple needle-shaped crystals were harvested after two days.

*[Tl(TCNQI$_2$)] (**4**)*: A sample of [Li(TCNQI$_2$)] (0.051 g, 0.1 mmol) was dissolved in methanol (10 mL) and $TlPF_6$ (0.035 g, 0.1 mmol) was dissolved in a 15 mL mixture of methanol/water (2:1 v/v). The two solutions were layered in a 6 mm O.D. thin tube. Dark-purple block-shaped crystals formed by slow diffusion over the course of two days.

*[Tl(TCNQ)] phase III (**5**)*: Quantities of $Bu_4N(TCNQ)$ (0.044 g, 0.1 mmol) and $TlPF_6$ (0.035 g, 0.1 mmol) were dissolved in acetonitrile (10 mL) and the solution was stirred for 2 h. The resulting precipitate was collected by filtration and dried in vacuo. Yield: 99%; elemental analysis calcd (%) for $C_{12}H_2N_4Tl$: C 35.28, H 0.99, N 13.71; found: C 34.68, H 0.86, N 13.41. Single crystals were obtained by separately dissolving $Bu_4N(TCNQ)$ (0.022 g, 0.05 mmol) and $TlPF_6$ (0.035 g, 0.1 mmol) in acetonitrile (5 and 10 mL, respectively) and carefully layering the solutions in a thin tube (6 mm O.D.). After slow diffusion over the course of a week, a very small crop of dark-purple dendritic needle-shaped crystals were obtained.

**Theoretical calculations**: The transfer integrals were calculated on the basis of the molecular-orbital calculations. The frozen orbital approximation was adopted and the intermolecular overlap integrals were evaluated from the overlap of the Slater orbitals by using the extended Hückel Slater exponents to consider the intermolecular interaction correctly.[24–26] The transfer integrals ($t$) were estimated by $t = E \times S$, for which $S$ is the overlap integrals of LUMOs between the TCNQ molecules, and $E$ is assumed to be −10 eV as the energy of the molecular orbital. The organic–metal interactions were estimated similarly to the transfer integrals between the TCNQ LUMO and the Tl6s orbital. The electronic configuration of a $Tl^+$ ion is $6s^26p^0$, so the 6s level is occupied. Because the Tl6p levels (−5.0 eV) are located far above the TCNQ LUMO (−11 eV), the transfer integrals to the Tl6s orbitals (−11.6 eV) are considered.

## Acknowledgements

The PI K.R.D. gratefully acknowledges the National Science Foundation for support under grant (CHE-0911354) and for equipment grants to purchase the CCD X-ray equipment (CHE-9807975) and the SQUID magnetometer (NSF-9974899). We also wish to thank Texas A&M University for additional financial support and the Advanced Photon Source at Argonne National Lab for facility support. Use of the Advanced Photon Source at Argonne National Laboratory was supported by the U. S. Department of Energy, Office of Science, Office of Basic Energy Sciences, under Contract No. DE-AC02–06CH11357. The data collected at Argonne National Laboratories were supported by the proposal GUP 13132.

[1] R. M. Metzger, *Chem. Rev.* **2003**, *103*, 3803–3834.
[2] O. Sato, J. Tao, Y. Zhang, *Angew. Chem.* **2007**, *119*, 2200–2236; *Angew. Chem. Int. Ed.* **2007**, *46*, 2152–2187.
[3] O. Sato, T. Kawakami, M. Kimura, S. Hishiya, S. Kubo, Y. Einaga, *J. Am. Chem. Soc.* **2004**, *126*, 13176–13177.
[4] a) J. M. Manriquez,, G. T. Yee,, R. S. McLean, A. J. Epstein, J. S. Miller, *Science* **1991**, *252*, 1415–1417; b) B. G. Morin, P. Zhou, C. Hahm, A. J. Epstein, J. S. Miller, *J. Appl. Phys.* **1993**, *73*, 5648–5650; c) P. Zhou, S. M. Long, J. S. Miller, A. J. Epstein, *Phys. Lett. A* **1993**, *181*, 71–79; d) J. S. Miller, A. J. Epstein, *Synth. Met.* **1993**, *56*, 3291–3298; e) P. Zhou, J. S. Miller, A. J. Epstein, *Phys. Lett. A* **1994**, *189*, 193–198; f) K. I. Pokhodnya, A. J. Epstein, J. S. Miller, *Adv. Mater.* **2000**, *12*, 410–413.
[5] a) R. Kato, H. Kobayashi, A. Kobayashi, *J. Am. Chem. Soc.* **1989**, *111*, 5224–5232; b) M. Nakano, M. Kato, K. Yamada, *Physica B* **1993**, *186–188*, 1077–1079; c) F. O. Karutz, J. U. von Schütz, H. Wachtel, H. C. Wolf, *Phys. Rev. Lett.* **1998**, *81*, 140–143; d) H. Schmitt, J. U. von Schütz, H. Wachtel, H. C. Wolf, *Synth. Met.* **1997**, *86*, 2257–2258; e) J. U. von Schütz, D. Bauer, H. Wachtel, H. C. Wolf, *Synth. Met.* **1995**, *71*, 2089–2090; f) J. U. von Schütz, D. Gomez, H. Wachtel, H. C. Wolf, *J. Chem. Phys.* **1996**, *105*, 6538–6545; g) J. U. von Schütz, D. Gomez, H. Schmitt, H. Wachtel, *Synth. Met.* **1997**, *86*, 2095–2096.
[6] J. P. Ferraris, D. O. Cowan, V. Walatka, J. H. Perlstein, *J. Am. Chem. Soc.* **1973**, *95*, 948–949.
[7] D. E. Schafer, F. Wudl, G. A. Thomas, J. P. Ferraris, D. O. Cowan, *Solid State Commun.* **1974**, *14*, 347–351.
[8] J. M. Thomas, *Nature Phys. Sci.* **1973**, *244*, 56–57.
[9] R. S. Potember, T. O. Poehler, D. O. Cowan, *Appl. Phys. Lett.* **1979**, *34*, 405–407.
[10] R. S. Potember, T. O. Poehler, R. C. Benson, *Appl. Phys. Lett.* **1982**, *41*, 548–550.
[11] a) J. J. Hoagland, X. D. Wang, K. W. Hipps, *Chem. Mater.* **1993**, *5*, 54; b) Z. Gu, H. Wu, Y. Wei, J. Liu, *J. Phys. Chem.* **1993**, *97*, 2543–2545; c) S. Liu, Y. Liu, P. Wu, D. Zhu, *Chem. Mater.* **1996**, *8*, 2779; d) N. Gu, W. Lu, S. Pang, C. Yuan, Y. Wei, *Thin Solid Films* **1994**, *243*, 468–471; e) S. Liu, Y. Liu, D. Zhu, *Thin Solid Films* **1996**, *280*, 271–277; f) S. Wakida, Y. Ujihira, *Jpn. J. Appl. Phys.* **1988**, *27*, 1314–1316; g) Z. Y. Hua, G. R. Chen, *Vacuum* **1992**, *43*, 1019–1023.
[12] R. A. Heintz, H. Zhao, X. Ouyang, G. Grandinetti, J. Cowen, K. R. Dunbar, *Inorg. Chem.* **1999**, *38*, 144–156.
[13] a) C. Di, G. Yu, Y. Liu, Y. Guo, W. Wu, D. Wei. D. Zhu, *Phys. Chem. Chem. Phys.* **2008**, *10*, 2302; b) X. Zhou, S. Wei, S. Zhang, *Langmuir* **2008**, *24*, 4464–4466; c) J. Billen, S. Steudel, R. Müller, J. Genoe, P. Heremans, *Appl. Phys. Lett.* **2007**, *91*, 2635071–3; d) A. K. Neufeld, I. Madsen, A. M. Bond, C. F. Hogan, *Chem. Mater.* **2003**, *15*, 3573–3585; e) D. J. Flannigan, V. A. Lobastov, A. H. Zewail, *Angew. Chem.* **2007**, *119*, 9366–9370; *Angew. Chem. Int. Ed.* **2007**, *48*, 9206–9210; f) K. Xiao, J. Tao, Z. Pan, A. A. Puretzky, I. N. Ivanov, S. J. Pennycook, D. B. Geohegan, *Angew. Chem.* **2007**, *119*, 2704–2708; *Angew. Chem. Int. Ed.* **2007**, *46*, 2650–2654.
[14] a) D. S. Acker, W. R. Hertler, *J. Am. Chem. Soc.* **1962**, *84*, 3370–3374; b) L. R. Melby, R. J. Harder, W. R. Hertler, W. Mahler, R. E. Benson, W. E. Mochel, *J. Am. Chem. Soc.* **1962**, *84*, 3374–3387.
[15] a) J. G. Vegter, T. Hibma, J. Kommandeur, *Chem. Phys. Lett.* **1969**, *3*, 427–429; b) N. Sakai, I. Shirotani, S. Minomura, *Bull. Chem. Soc. Jpn* **1972**, *45*, 3321–3328; c) H. Terauchi, *Phys. Rev. B* **1978**, *17*, 2446–2452.
[16] A. Hoekstra, T. Spoelder, A. Vos, *Acta Crystallogr. B* **1972**, *28*, 14–25.
[17] I. Shirotani, H. Kobayashi, *Bull. Chem. Soc. Jpn.* **1973**, *46*, 2595–2596.
[18] B. Van Bodegom, J. L. De Boer, A. Vos, *Acta Crystallogr. B* **1977**, *33*, 602–604.
[19] a) R. J. Janssen, M. P. T. Christiaans, C. Hare, N. Martin, N. S. Sariciftci, A. J. Heeger, F. Wudl, *J. Chem. Phys.* **1995**, *103*, 8840–8845; b) H. Miyata, Y. Tatewaki, T. Akutagawa, T. Hasegawa, T. Nakamura, C. A. Christensen, J. Becher, *Thin Solid Films* **2003**, *438–439*, 1–6.
[20] N. Lopez, H. Zhao, A. Ota, A. V. Prosvirin, E. W. Reinheimer, K. R. Dunbar, *Adv. Mater.* **2010**, *22*, 986–989.
[21] S. Hünig, H. Meixner, T. Metzenthin, U. Langohr, J. U. von Schütz, H. C. Wolf, E. Tillmanns, *Adv. Mater.* **1990**, *2*, 361–363.
[22] G. Bouhadir, D. Bourissou, *Chem. Soc. Rev.* **2004**, *33*, 210–217.

  

[23] C. Avendano, Z. Zhang, A. Ota, H. Zhao, K. R. Dunbar, *Angew. Chem.* **2011**, *123*, 6673–6677; *Angew. Chem. Int. Ed.* **2011**, *50*, 6543–6547.
[24] a) R. Hoffmann, *J. Chem. Phys.* **1964**, *40*, 2474–2479; b) R. Hoffmann, *J. Chem. Phys.* **1964**, *40*, 2480–2488; c) R. Hoffmann, *J. Chem. Phys.* **1964**, *40*, 2745.
[25] T. Mori, A. Kobayashi, Y. Sasaki, H. Kobayashi, G. Saito, H. Inokuchi, *Bull. Chem. Soc. Jpn.* **1984**, *57*, 627–633.
[26] L. A. Bengtsson, R. Hoffmann, *J. Am. Chem. Soc.* **1993**, *115*, 2666–2676.
[27] L. Shields, *J. Chem. Soc. Faraday Trans. 2* **1985**, *81*, 1–9.
[28] M. Konno, T. Ishii, Y. Saito, *Acta Crystallogr. B* **1977**, *33*, 763–770.
[29] M. Konno, Y. Saito, *Acta Crystallogr. B* **1975**, *31*, 2007–2012.
[30] R. Kumai, Y. Okimoto, Y. Tokura, *Science* **1999**, *284*, 1645–1647.
[31] K. Akhbari, A. Morsali, *Coord. Chem. Rev.* **2010**, *254*, 1977–2006.
[32] A. V. Mudring, F. Rieger, *Inorg. Chem.* **2005**, *44*, 6240–6243.
[33] A. Askarinejad, A. A. Torabi, A. Morsali, *Z. Naturforsch. B* **2006**, *61*, 565–569.
[34] R. Hoffmann, *J. Chem. Phys.* **1963**, *39*, 1397–1412.
[35] M.-H. Whangbo, R. Hoffmann, *J. Am. Chem. Soc.* **1978**, *100*, 6093–6098.
[36] T. Mori, M. Katsuhara, *J. Phys. Soc. Jpn.* **2002**, *71*, 826–844.
[37] S. Shitzkovsky, M. Weger, H. Gutfreund, *J. Phys. France* **1978**, *39*, 711–718.
[38] R. Kato, S. Aonuma, H. Sawa, *Synth. Met.* **1995**, *70*, 1071–1074.

Received: September 24, 2012
Published online: ■■ ▮▮, 0000

  

**Main-group semiconductors**: New 2,5-dihalogen-substituted [Tl(TCNQX$_2$)] (TCNQ7,7,8,8-tetracyanoquinodimethane, X = H, Cl, Br, I) derivatives reveal potential for the realization of unprecedented molecule-based main-group semiconductors (see figure). The theoretical simulation of band structures hints at modulation of the 1D band structure by the $Tl^{I}$ cations.

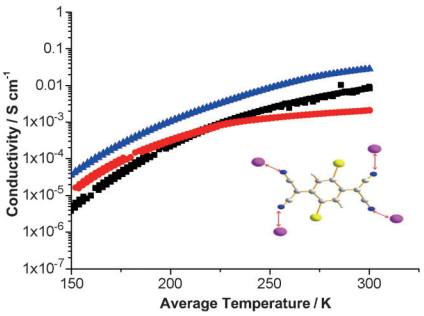


Semiconductors